

1 Autumn – winter minimum temperature changes in the 2 southern Sikhote-Alin mountain range of northeast Asia since 3 1529 AD

4 Olga N. Ukhvatkina, Alexander M. Omelko, Alexander A. Zhmerenetsky, Tatyana Y. Petrenko.

5
6 Federal Scientific center of the East Asia terrestrial biodiversity Far Eastern Branch of Russian
7 Academy of Sciences, Vladivostok 690022 RUSSIA

8
9 *Correspondence to:* Olga Ukhvatkina (ukhvatkina@gmail.com)
10

11 **Abstract.** The aim of our research was to reconstruct climatic parameters (for the first time for the Sikhote-Alin
12 mountain range) and to compare them with global climate fluctuations. As a result, we have found that one of the
13 most important limiting factors for the study area is the minimum temperatures of the previous autumn-winter
14 season (August-December), and this finding perfectly conforms to that in other territories. We reconstructed the
15 previous August-December minimum temperature for 485 years, from 1529 to 2014. We found twelve cold periods
16 (1535-1540, 1550-1555, 1643-1649, 1659-1667, 1675-1689, 1722-1735, 1791-1803, 1807-1818, 1822-1827, 1836-
17 1852, 1868-1887, 1911-1925) and seven warm periods (1560-1585, 1600-1610, 1614-1618, 1738-1743, 1756-1759,
18 1776-1781, 1944-2014). These periods correlate well with reconstructed data for the Northern Hemisphere and the
19 neighboring territories of China and Japan. Our reconstruction has 3, 9, 20 and 200-year periods, which are may be
20 in line with high-frequency fluctuations in ENSO, the short-term solar cycle, PDO fluctuations and the 200-year
21 solar activity cycle, respectively. We suppose that the temperature of North Pacific, expressed by Pacific Decadal
22 Oscillation may make a major contribution to regional climate variations. We also assume that the regional climatic
23 response to solar activity becomes apparent in the temperature changes in the northern part of Pacific Ocean and
24 corresponds to cold periods during the solar minimum. These comparisons show that our climatic reconstruction
25 based on tree-ring chronology for this area may potentially provide a proxy record for long-term, large-scale past
26 temperature patterns for northeast Asia. The reconstruction reflects the global traits and local variations in the
27 climatic processes of the southern territory of the Russian Far East for more than the past 450 years.

28 1 Introduction

29 Global climate change is the main challenge for human life and natural systems, which is why we should clearly
30 understand climatic changes and their mechanisms. A retrospective review of climatic events is necessary for
31 understanding the climatic conditions from a long-term perspective. At the same time, instrumental climate
32 observations rarely cover more than a 100-year period and are often restricted to 50-70 years. This restriction forces
33 the researchers to continuously find new ways and methods to reconstruct climatic fluctuations. Dendrochronology
34 has been widely applied in climatic reconstruction for local territories and at the global scale for both climatic
35 reconstructions of the past few centuries and paleoclimatic reconstructions because it is rather precise, extensively
36 used and a replicable instrument (Corona et al.; Popa and Bouriaund, 2014; Kress et al., 2014; Lyu et al., 2016).
37 A great number of studies have focused on climatic change reconstruction for the northeastern parts of China based
38 on *P. koraeinsis* radial growth studies (e.g., Zhu et al., 2009; Wang et al., 2013; Wang et al., 2016; Zhu et al., 2015;
39 Lyu et al. 2016). Climatic parameters were reconstructed for the whole Northern Hemisphere (Wilson et al., 2016),
40 China (Ge et al., 2016), and temperature characteristics were reconstructed for northeastern Asia (Ohyama et al.,
41 2013). Despite this, there are very few studies of Russian Far East climate (e.g., Willes et al., 2014; Jacoby et al.,

2004; Shan et al., 2015); moreover, there is an absence of dendrochronological studies for the continental part of Russian Far East. Meanwhile, most of species present in northeastern China, the Korean peninsula and Japan grow in this region. In addition, the distribution areas of these trees often end in the south of the Russian Far East, which increases the climatic sensitivity of plants. Additionally, some parts of the forests in the Russian Far Eastern have not been subjected to human activity for the last 2000-4000 years. This makes it possible to forests extend the studied timespan. In addition, the southern territory of the Russian Far East is sensitive to global climatic changes as it is under the influence of cold air flow from northeastern Asia during the winter and summer monsoons. All of the factors listed above create favorable conditions for dendroclimatic studies.

It is well-known that cold and warm periods of the climate is correlated with intensive solar activity (e.g., the Medieval Warm Period), while decreases in temperature occurs during periods of low solar activity (e.g., the Little Ice Age; Lean and Rind, 1999; Bond et al., 2001). According to findings from an area of China neighboring the territory studied here, the registered warming has been significantly affected by global warming since the 20th century (Ding and Dai, 1994; Wang et al., 2004; Zhao et al., 2009), which is often indicated by a faster rise in night or minimum temperatures (Karl et al., 1993; Ren and Zhai, 1998; Tang et al., 2005). To better understand and evaluate future temperature change trends, we should study the long-term history of climatic changes.

However, using tree-ring series for northeastern Asia (particularly temperature) is rather complicated due to the unique hydrothermal conditions of the region. Most reconstructions cover periods of less than 250 years (e.g., Shao and Wu, 1997; Zhu et al., 2009; Wang et al., 2012; Li and Wang, 2013; Yin et al., 2009; Zhu et al., 2015), except for a few with periods up to 400 years (Lyu et al., 2016; Wiles et al., 2014). The short period of reconstructions is the reason why such reconstructions cannot capture low-frequency climate variations.

The warming of the climate (particularly minimum temperature increase) is registered across the whole territory of northeastern Asia (Lyu et al., 2016). In the Russian Far-East, such warming has been recorded for more than 40 past years (Kozhevnikova, 2009). However, the lack of detailed climatic reconstructions for the last few centuries makes it difficult to capture long-period climatic events for this territory and interpret the temperature conditions for the last 500-1000 years.

Therefore, the main objectives of this study were (1) to develop the first three-ring-width chronology for the southern part of the Russian Far East; (2) to analyze the regime of temperature variation over the past centuries in the southern part of the Russian Far East; (3) to identify the recent warming amplitude in context of long-term changes and to analyze the periodicity of climatic events and their driving forces. Our new minimum temperature record supplements the existing data for northeast Asia and provides new evidence of past climate variability. There is the potential to better understand future climatic trajectories from these data in northeast Asia.

2 Materials and methods

2.1 Study area

We studied the western macroslope of the southern part of the Sikhote-Alin mountain range (Southeastern Russia) at the Verkhneussuriysky Research Station of the Federal Scientific Center of the East Asia terrestrial biodiversity Far East Branch of the Russian Academy of Sciences (4400 ha; N 44°01'35.3'', E 134°12'59.8'', Fig. 1).

The territory is characterized by a monsoon climate with relatively long, cold winters and warm, rainy summers. The average annual air temperature is 0.9 °C; January is the coldest month (−32 °C average temperature), and July is the warmest month (27 °C average temperature). The average annual precipitation is 832 mm (Kozhevnikova, 2009). Southerly and southeasterly winds predominate during the spring and summer, while northerly and northwesterly

83 winds predominate in autumn and winter. The terrain includes mountain slopes with an average angle of $\sim 20^\circ$, and
84 the study area is characterized by brown mountain forest soils (Ivanov, 1964) (Fig. 2).
85 Mixed forests with Korean pine (*Pinus koraiensis* Siebold et Zucc.) are the main vegetation type in the study area,
86 and they form an altitudinal belt up to 800 m above sea level. These trees are gradually replaced by coniferous fir-
87 spruce forests at high altitudes (Kolesnikov, 1956). Korean pine-broadleaved forests are formed by up to 30 tree
88 species, with *Abies nephrolepis* (Trautv.) Maxim, *Betula costata* (Trautv.) Regel., *Picea jezoensis* (Siebold et Zucc.)
89 Carr., *P. koraiensis* and *Tilia amurensis* Rupr. being dominant.
90 Korean pine-broadleaved forests are the main forest vegetation type in the Sikhote-Alin mountain range in the
91 southern part of the Russian Far East. This area is the northeastern limit of the range of Korean pine-broadleaved
92 forests, which are also found in northeastern China (the central part of the range), on the Korean peninsula, and in
93 Japan. The Sikhote-Alin mountain range is one of the few places where significant areas of old-growth Korean pine-
94 broadleaved forest remain. In the absence of volcanic activity, which is a source of strong natural disturbances in the
95 central part of the range (Liu, 1997; Ishikava, 1999; Dai et al., 2011), wind is the primary disturbance factor on this
96 territory. Wind causes a wide range of disturbance events, from individual treefalls to large blowdowns (Dai et al.,
97 2011).
98 Approximately 60% of the Research Station area had been subjected to selective clear-cutting before the station was
99 established in 1972. The remaining 40% of its area has never been clear-cut and is covered by unique old-growth
100 forest.

101 2.2 Tree-ring chronology development

102 Our study is based on data collected in a 10.5-ha permanent plot (Omelko and Ukhvatkina, 2012; Omelko et al., 2016),
103 which was located in the middle portion of a west-facing slope with an angle of 22° at a gradient altitude 750-950 m
104 above sea level. The forest in the plot was a late-successional stand belonging to the middle type of Korean pine-
105 broadleaved forests at the upper bound of the distribution of Korean pine, where it forms mixed stands of Korean
106 pine-spruce and spruce-broadleaved forests (Kolesnikov, 1956).
107 One core per undamaged old-growth mature tree (25 cores from 25 trees) and one sample from dead trees (20 samples)
108 were extracted from *P. koraiensis* trees in the sample plots from the trunks at breast height. In the laboratory, all tree-
109 ring samples were mounted, dried and progressively sanded to a fine polish until individual tracheids within annual
110 rings were visible under an anatomical microscope according to standard dendrochronological procedures (Fritts,
111 1976; Cook and Kairiukstis, 1990). Preliminary calendar years were assigned to each growth ring, and possible errors
112 in measurement due to false or locally absent rings were identified using the Skeleton-plot cross-dating method
113 (Stokes and Smiley, 1968). The cores were measured using the semi-automatic Velmex measuring system (Velmex,
114 Inc., Bloomfield, NY, USA) with a precision of 0.01 mm. Then, the COFECHA program was used to check the
115 accuracy of the cross-dated measurements (Holmes, 1983). To mitigate the potential trend distortion problem in
116 traditionally detrended chronology (Melvin and Briffa, 2008; Anchukaitis et al., 2013), we used a signal-free method
117 (Melvin and Briffa, 2008) to detrend the tree-ring series using the RCSigFree program (<http://www.ldeo.columbia.edu/tree-ring-laboratory/resources/software>).
118
119 Age-related trends were removed from the raw tree-ring series using an age-dependent spline smoothing method. The
120 ratio method was used to calculate tree-ring indices, and the age-dependent spline was selected to stabilize the variance
121 caused by core numbers. Finally, the stabilized signal-free chronology was used for the subsequent analysis (Fig. 3).
122 The mean correlations between trees (*Rbt*), mean sensitivity (MS) and expressed population signal (EPS) were
123 calculated to evaluate the quality of the chronology (Fritts, 1976). *Rbt* reflects the high-frequency variance, and MS

124 describes the mean percentage change from each measured annual ring value to the next (Fritts, 1976; Cook and
125 Kairiukstis, 1990). EPS indicates the extent to which the sample size is representative of a theoretical population with
126 an infinite number of individuals. A level of 0.85 in the EPS is considered to indicate a chronology of satisfactory
127 quality (Wigley *et al.*, 1984). The statistical characteristics of the chronology are listed in Table 1.

128 The full length of the chronology spans (VUS chronology) from 1451 to 2015. A generally acceptable threshold of
129 the EPS was consistently greater than 0.85 from AD 1602 to 2015 (9 trees; Fig. 3b), which affirmed that this is a
130 reliable period. However, although the EPS value from AD 1529 to 1602 was less than 0.85, it matches a minimum
131 sample depth of 4 trees in this segment (EPS>0.75). Although the record from AD 1529 to 1602 is thus less certain,
132 we here report it as it is very important to extend the tree-ring chronology as much as possible because there are only
133 a few long climate reconstructions in this area. Therefore, we retained the part from 1529 to 1602 in the reconstruction.

134 2.3 Climate data and statistical methods

135 Monthly precipitation, monthly mean and minimum temperature data were obtained from the Chuguevka
136 meteorological station (44.151462 N, 133.869530 E, about 30 km from Verkhneussuriisky research station) and the
137 meteorological post at the Verkhneussuriisky research station of the Federal Scientific Center of the East Asia
138 terrestrial biodiversity FEB RAS (Meteostation 7 – MP7) as well. The periods of monthly data available from the
139 Chuguevka and Verkhneussuriisky stations are 1936-2004 and 1969-2004, respectively (1971-2003 for minimum
140 temperature data from the Chuguevka).

141 The data of large-scale climate conditions, such as the Northern Hemisphere temperature (NH), North Atlantic
142 Oscillation (AMO), Pacific Decadal Oscillation (PDO) and Nino3 reconstruction (Mann *et al.*, 2009), and also
143 indicators of solar activity, such as reconstructed solar constant (TSI, Lean, 2000) and sun spot number (SSN) were
144 downloaded and analyzed in Royal Netherlands Meteorological Institute climate explorer (<http://climexp.knmi.nl>).

145 To demonstrate that our reconstruction representative and reflect temperature variations, we conducted spatial
146 correlation between our temperature reconstruction and gridded temperature dataset of the Climate Research Unit
147 (CRU TS4.00) for the period 1960-2003, by using the Royal Netherlands Meteorological Institute climate explorer
148 (<http://climexp.knmi.nl>).

149 2.4 Statistical analyses

150 A correlation analysis was used to evaluate the relationships between the ring-width index and observed monthly
151 climate records from the previous June to the current September. To identify the climate-growth relationships of
152 Korean pine in the southern Sikhote-Alin mountain range, a Pearson's correlation was performed between climate
153 variables and tree-width index. We used a traditional split-period calibration/verification method to explore the
154 temporal stability and reliability of the reconstruction model (Fritts, 1976; Cook and Kairiukstis, 1990). The Pearson's
155 correlation coefficient (r), R-squared (R^2), the reduction of the error (RE) the coefficient of efficiency (CE), and the
156 product means test (PMT) were used to verify the results. Analyses were carried out in R using the treeclim package
157 (Zang and Biondi, 2015) and STATISTICA software (StatSoft®). Analyses of reconstruction included multi-taper
158 method (MTM) (Mann & Lees, 1996) and Monte Carlo Singular Spectrum Analysis (SSA; Allen and Smith, 1996).
159 Analysis was carried out in SSA-MTM Toolkit for Spectral Analysis software (Ghil *et al.*, 2001; Dettinger *et al.*,
160 1995).

161 3 Results

162 3.1 Climate-radial growth relationship

163 Relationships between the VUS chronology and monthly climate data are shown in Fig 4. To reveal the correlation
164 between climatic parameters and radial growth change of *P. koraiensis*, we had three data sets: the first-time series
165 had a length of 68 years (1936-2004, Chuguevka), the second had a length of 34 years (1966-2000, MP7), and the
166 third had a length of 33 years (1971-2003, Chuguevka, minimum temperature). To select the appropriate parameters,
167 we analyzed all datasets. As a result, we revealed a reliable but slight positive correlation between *P. koraiensis* growth
168 and precipitation in May and June of the current year and September of the previous year in the territory of Chuguevka
169 village (Fig. 4a). There is also a slight positive correlation with precipitation in September of the previous year and
170 May of the current year at Metheostation 7 (MP7) (Fig. 4b). In addition, we revealed a slight negative correlation with
171 precipitation in February-March of the current year.

172 As for the correlation between temperature and *P. koraiensis* growth, the analysis reveals a weak positive correlation
173 with the average monthly temperature in June of the previous year and in February-April of the current year in the
174 Chuguevka settlement and a slight negative correlation with the average monthly temperature in June-July as well
175 (Fig. 4c). The analysis of the correlation with the average monthly temperature at Metheostation 7 (MP7) shows us a
176 weak positive correlation with temperature in August and December of the preceding year and a negative correlation
177 with temperature in July of the current year (Fig. 4d). In addition, we analyzed the correlation with minimum average
178 monthly temperatures at MP7 and Chuguevka. The revealed correlation with minimum temperature is reliable but
179 weak (Fig. 4e,f).

180 Moreover, based on the weak interaction that was revealed, we analyzed the correlation with climatic parameters for
181 selected ranges of months (Fig. 4h,g). The highest significant correlation appears between growth and the minimum
182 monthly temperature of August-December of the previous year at Chuguevka (Fig. 4h), on which we base our
183 subsequent reconstructions.

184 3.2 Minimum temperature reconstruction

185 Basing on analysis of the correlation between climatic parameters and Korean pine growth, we constructed a linear
186 regression equation to reconstruct the minimum monthly temperature of August-December of the previous year
187 (VUSr). The transfer function was as follows:

$$188 \text{VUSr} = 7.189X_t - 15.161$$

$$189 (N=32, R=0.620, R^2=0.385, R^2_{\text{adj}}=0.364, F=18.76, p < 0.001)$$

190 where VUSr is the August-December minimum temperature at Chuguevka and X is the tree-ring index of the Korean
191 pine RSC chronology in year t . The comparison between the reconstructed and observed mean growing season
192 temperatures during the calibration period is shown in Fig. 5(a). The cross-validation test for the calibration period
193 (1971-1997, $R=0.624$) yielded a positive RE of 0.334, a CE of 0.284, and the cross-validation test for calibration
194 period 1977-2003 ($R=0.542$) a positive RE of 0.654, a CE of 0.644, confirming the predictive ability of the model.
195 Although during the study period, the model shows the observed values very well, the short observation period (1971-
196 2003) does not allow using split-sampling calibration and verification methods in full for evaluating quality and model
197 stability. This limitation is why we used a bootstrapping resampling approach (Efron, 1979; Young, 1994) for stability
198 evaluation and transfer function precision. The idea that this method is based on indicates that the available data
199 already include all the necessary information for describing the empirical probability for all statistics of interest.
200 Bootstrapping can provide the standard errors of statistical estimators even when no theory exists (Lui et al., 2009).
201 The calibration and verification statistics are shown in Table 2. The statistical parameters used in bootstrapping are

202 very similar to those from the original regression model, and this proves that the model is quite stable and reliable and
203 that it can be used for temperature reconstruction.

204

205 **3.3 Temperature variations from AD 1529 to 2014 and temperature periodicity**

206 Variations in the reconstructed average minimum temperature of the previous August-December (VUSr) since AD
207 1529 and its 21-year moving average are shown in Fig. 5b. The 21-year moving average of the reconstructed series
208 was used to obtain low-frequency information and analyze temperature variability in this region. The mean value of
209 the 486-year reconstructed temperature was -7.93°C with a standard deviation of $\pm 1.40^{\circ}\text{C}$. We defined warm and
210 cold periods as when temperature deviated from the mean value plus or minus 0.5 times the standard deviation,
211 respectively (Fig. 5b). If the reconstructed minimum temperatures were above or below the average value by $>0.5\text{ SD}$
212 for three or more years, then we considered this deviation as warm or cold period, respectively. Also, if two warm (or
213 cold) periods were separated by one year, when the temperature sharply decreased (or increased), then such periods
214 merged into one.

215 Hence, warm periods occurred in 1560-1585, 1600-1610, 1614-1618, 1738-1743, 1756-1759, 1776-1781, 1944-2014,
216 and cold periods appeared in 1535-1540, 1550-1555, 1643-1649, 1659-1667, 1675-1689, 1722-1735, 1791-1803,
217 1807-1818, 1822-1827, 1836-1852, 1868-1887, 1911-1925. Among them, the four warmest years were in 1574 ($-$
218 4.35°C), 1606 (-5.35°C), 1615 (-5.71°C), 1741 (-5.36°C), 1757 (-6.16°C), 1779 (-5.21°C), 2008 (-2.72°C), while
219 the three coldest year were in 1543 (-9.84°C), 1551 (-9.88°C), 1647 (-10.77°C), 1662 (-11.10°C), 1685 (-9.45°C),
220 1728 (-10.08°C), 1799 (-10.70°C), 1815 (-10.13°C), 1825 (-9.87°C), 1843 (-10.55°C), 1883 (-10.73°C), 1913 ($-$
221 10.29°C). The longest cold period extended from 1868 to 1887, and the longest warm period extended from 1944 to
222 present day. The coldest year is 1662 (-11.10°C) and the warmest year is 2008 (-2.72°C).

223 The MTM spectral analysis over the full length of our reconstruction revealed significant ($p < 0.05$) cycle peaks at
224 2.3-year (95%), 2.5-year (99%), 2.9-year (99%), 3.0-year (99%), 3.3-year (95%), 3.7-year (95%), 8.9-year (99%)
225 short periods and 20.4-year (95%), 47.6-year (95%), 188.7-year (99%) long periods (Fig. 6). Singular spectrum
226 analysis (SSA) reveals 8 leading temporal modes that significant at the 95% confidence level (Allen & Smith, 1996).
227 Of these, SSA analysis reveals a single significant low order mode variability near 200 years, but there is little evidence
228 in the reconstruction variability at the 40-50 years. Also 3 significant power periods were reveals: 20.4-year, 9-year
229 and near 3-year periods. Comparison of the reconstruction and global temperature for oceans of Northern Hemisphere
230 (NH), North Atlantic Oscillation (AMO), Pacific Decadal Oscillation (PDO) and Nino3 reconstruction (Mann et al.,
231 2009) show significant correlation between reconstruction and NH ($r=0.67$, $p<0.0001$), AMO ($r=0.49$, $p<0.001$), and
232 PDO ($r=0.68$, $p<0.0001$), and non-significant correlation between reconstruction and Nino3 reconstruction ($r=0.27$,
233 $p=0.08$). Comparison of the reconstruction and indicators of solar activity shows significant correlation of the
234 minimum temperature with the TSI ($r=0.52$, $p<0.0001$) and non-significant correlation with SSN ($r=0.26$, $p<0.1$).
235 Comparison of the instrumental climate data and instrumental indicators of solar activity shows significant correlation
236 of the minimum temperature with the TSI ($r=0.52$, $p<0.0001$) and non-significant correlation with SSN ($r=0.26$,
237 $p<0.1$).

238 Spatial correlations between our reconstruction and the CRU TS4.00 temperature dataset reveal our record's
239 geographical representation (Fig. 7). The results show that the reconstruction of mean minimum temperature of
240 previous August – December is significantly positively correlated with the CRU TS4.00 ($r=0.568$, $p<0.0001$).

241 **4 Discussion**

242 **4.1 Climate-growth relationships**

243 The results of our analysis suggest that the radial growth of Korean pine in the southern part of the Sikhote-Alin
244 mountain range is mainly limited by the pre-growth autumn-winter season temperatures, in particular the minimum
245 temperatures of August-December (Fig. 4). It is widely known that tree-ring growth in cold and wet ecotopes, situated
246 on sufficiently high elevation in the Northern Hemisphere, strongly correlate with temperature variability in large
247 areas of Asia, Eurasia, North America (Zhu et al., 2009; Anchukaitis et al., 2013; Thapa et al., 2015; Wiles et al.,
248 2014). The limiting influence of temperature on *P. koraiensis* growth has been mentioned in many studies (Wang et
249 al., 2016; Yin et al., 2009; Wang et al., 2013; Zhu et al., 2009). However, the temperature has various limiting effects
250 in different conditions, and these limiting effects manifest in different ways (Wang et al., 2016). For example, Zhu et
251 al., 2016 indicates that in more northern and arid conditions of the Zhangguangcai Mountains, while precipitation is
252 not the main limiting factor, precipitation is considerably below evaporation during the growth season. This finding
253 is why a stable correlation between *P. koraiensis* growth and the growth season temperature is revealed. This finding
254 is also why moisture availability in soil might be the main limiting factor for Korean pine growth (Zhu et al., 2016),
255 but the emergence of this circumstance can be different in different conditions.

256 The correlation between growth and minimum temperatures in August-December of the previous year, as revealed
257 in our research, was also mentioned for Korean pine in other works (Wang et al., 2016; Zhang et al., 2015). This
258 finding may be explained by the following circumstances. Extreme temperatures limit the growth of trees at the tree
259 line or in high-latitude forests (Wilson and Luckman, 2002; Körner and Paulsen, 2004; Porter et al., 2013; Yin et al.,
260 2015). Taking into consideration the fact that the study area is situated at the altitudinal limit of Korean pine forest
261 distributions, in particular the Korean pine (Kolesnikov, 1956), these findings seem to be reliable.

262 In addition, in the conditions close to extreme for this species, low temperatures in autumn-winter may lead to thicker
263 snow cover, which melts far more slowly in spring (Zhang et al., 2015). The study area is notable for its dry spring,
264 and the amount of precipitation is minimal during the most important period of tree-growth in April-May
265 (Kozhevnikova, 2009). If the vegetation period of the plant cannot begin at the end of March and packed snow cover
266 melting is impeded up until the beginning of May, plant growth may be reduced. Moreover, although cambial activity
267 stops in the winter, organic components are still synthesized by photosynthesis. Low temperatures (in the territory of
268 the VUSr it can reach -48°C in certain years) may induce to loss of accumulated materials, which adversely affects
269 growth (Zhang et al., 2015). The study area is in the center of the vegetated area, where the conditions for Korean
270 pine growth are optimal during the growing season, and only minimum temperature is regarded as an extreme factor.

271 **4.2 Comparison with other tree-ring-based temperature reconstructions**

272 At present, temperature reconstructions are uncommon for the Russian Far East, and research sites are located for
273 thousands of kilometers away from one another. For example, Wiles et al. undertook a study of summer temperatures
274 on Sakhalin Island (Wiles et al., 2014). Unfortunately, it is impossible to compare our findings with theirs because
275 Sakhalin Island is climatically far more similar to Japanese islands than to the Sikhote-Alin mountains, and
276 temperature variations in their study area are mainly caused by oceanic currents.

277 In addition, instrumental observations from the study area rarely encompass a period longer than 50 years (and studies
278 have only been conducted for large settlements). Consequently, the tree-ring record serves as a good indicator of the
279 past cold-warm fluctuations in the Russian Far East. The analysis of spatial correlations between our reconstruction

280 and the CRU TS4.00 temperature dataset reveal spatial correlations between the observed and reconstruction
281 minimum temperatures from the CRU TS4.00 gridded T_{\min} dataset during the baseline period of 1960-2003 (Fig. 7).
282 It's indicating that our temperature reconstruction is representative of large-scale regional temperature variations and
283 can be taken as representative of southeastern of the Russian Far East and northeastern of the China.

284 To identify the regional representativeness of our reconstruction, we compared it with two temperature reconstructions
285 for surroundings areas (Fig. 1) and a reconstruction for the Northern Hemisphere (Fig. 8). The first reconstruction was
286 for summer temperatures in the Northern Hemisphere (Wilson et al., 2016; Fig. 1). The second reconstruction was an
287 April-July tree-ring-based minimum temperature reconstruction for Laobai Mountain (northeast China), which is
288 approximately 500 km northwest of our site. The third was a February-April temperature reconstruction for the
289 Changbai Mountain (Zhu et al., 2009; Fig. 1), which are approximately 430 km southwest of our site. Although the
290 spring and summer temperatures have been reconstructed in the last two cases, we use these reconstructions for
291 comparison, because, firstly, there are no other reconstructions for this region, and secondly, despite the possible
292 seasonal shifts, long cold and warm periods should be identified in all seasons.

293 Cold and warm periods are shown in table 3 (the duration is given by the authors of the article). The reconstructions
294 show that practically all cold and warm periods coincide but have different durations and intensities. The data on
295 Northern Hemisphere show considerable overlaps of cold and warm periods, and the correlation between
296 reconstructions is 0.45 ($p > 0.001$). At the same time, we found the warm period 1560-1585, which is not clearly
297 shown in reconstruction for the Northern Hemisphere, though the general trend of temperature change is maintained
298 during this period (Fig. 8). Long cold periods from 1643 to 1667 and 1675-1690 that were revealed for another territory
299 (Lyu et al., 2016; Wilson et al., 2016) coincided with the Maunder Minimum (1645–1715), an interval of decreased
300 solar irradiance (Bard et al., 2000). The coldest year in this study (1662) revealed in this period too. The Dalton
301 minimum period centered in 1810 is also notable. Interestingly that cold periods of 1807-1818, 1822-1827, 1836-1852
302 and 1868-1887 is also registered in reconstructions for Asia (Ohayama et al., 2013) and by Japanese researchers
303 (Fukaishi & Tagami, 1992; Hirano & Mikami, 2007). Moreover, instrumental observations reconstructed for western
304 Japanese territories (the nearest to the study area) provide evidence of a cold period in the 1830s-1880s with a short
305 warm spell in the 1850s (Zaiki et al., 2006), which is in agreement with our data (not reliably period 1855-1865, Tabl.
306 3). For this period, there are contemporaneous records of severe hunger in Japan in 1832 and 1839, which was the
307 result of a summer temperature decrease and rice crop failure (Nishimura & Yoshikawa, 1936).

308 In this case, the longer cold period for the study area can be explained by the relatively lower influence of the warm
309 current and monsoon and generally colder climate in the south of the Russian Far East compared with Japanese islands.
310 The differing opinion about the three cold periods in China in the 17th, 18th and 19th centuries (Wang et al., 2003) is
311 also corroborated by our reconstruction. The cold period in the 19th century is even more pronounced than that reported
312 by Lyu et al., 2016. Moreover, Lyu et al., 2016 corroborate that the ascertained cold period in 19th century is more
313 evident in South China, but it is less clear in the northern territories or has inverse trend. Although the Russian Far
314 East is further north than the southern Chinese provinces and is closer to the northern part of the country, the marked
315 monsoon climate likely made it possible to reflect the general cold trend in 19th century, which was typical both for
316 China and the entire Northern Hemisphere. Because of this possible explanation, the cold period in the 19th century
317 for the Changbai Mountains shows up more distinctly than for the northern and western territory of Laobai Mountain
318 (Fig. 8).

319 Apparently, this discrepancy in regional climate flow is the reason that our reconstruction agrees well with the general
320 reconstruction for the whole hemisphere ($r = 0.45, p < 0.001$) and to a lesser extent agrees with the regional curves for
321 Laobai Mountain ($r = 0.23, p < 0.001$) and Changbai Mountain ($r = 0.32, p < 0.001$).

322 The changing dynamics of the 20th century temperature is also interesting to watch. The comparison of the minimum
323 annual temperatures for the territory and the reconstructed data for the period of 1960-2003 shows significant data
324 correlation (Fig. 7), including the northeast part of China. At the same time, for Chinese territory (both for southwest
325 regions and for more northwestern regions), the warming is apparent only in the last quarter century (Zhu et al., 2009)
326 or at the end of the 20th century (Lyu et al., 2016) (Fig. 8 c,d). This trend, revealed for the southern Sikhote-Alin
327 mountains (a warm spell since 1944), is corroborated for the whole Northern Hemisphere (Wison et al., 2016) (Fig.
328 8a,b). The maximum cold period is also corroborated, which we note for the 19th century (Fig. 8a,b).

329 The probable explanation is in the regional climate flow differences in the compared data. The territory of northeastern
330 China is more continental, though the influence of the Pacific Ocean is also notable. At the same time, the southern
331 part of the Sikhote-Alin mountains is more prone to the influence of monsoons, as are the Japanese islands. According
332 to paleoreconstructions, the Little Ice Age occurred in the Northern Hemisphere 600-150 years ago (Borisova, 2014).
333 The period of landscape formation (vegetation types and altitudinal zonation) for the Sikhote-Alin range during the
334 transition from the Little Ice Age to contemporary conditions occurred within the last 230 years (Razzhigaeva et al.,
335 2016). The timeframe of the Little Ice Age is generally recognized as varying considerably depending on the region
336 (Bazarova et al., 2014). However, it is certain that the Little Ice Age is accompanied by an increase in humidity in
337 coastal areas of northeast Asia (Bazarova et al., 2014). Thus, in similar conditions on the Japanese islands, the Little
338 Ice Age was accompanied by lingering and intensive rains (Sakaguchi, 1983), and the last typhoon activity was
339 registered for the Japanese islands from the middle of the 17th century to the end of the 19th century (Woodruff et al.,
340 2009). At the same time, the reconstruction of climatic changes for the whole territory of China for the last 2000 years
341 (Ge et al., 2016) shows that the cold period lasted until 1920, which correlates with the data we obtained. This timespan
342 wholly coincides with our data, and we can draw the conclusion that in the southern region of the Sikhote-Alin
343 mountains, the Little Ice Age ended at the turn of the 19th century.

344 Unfortunately, when comparing temperature, different changes were also observed for some cold and warm years
345 (Fig. 8). This finding may be attributed to differences in the reconstructed temperature parameters (such as average
346 value, minimum temperature and maximum temperature) and environmental conditions in different sampling regions.
347 Recent studies show that the oscillations in the medium, minimum and maximum temperature are often asymmetrical
348 (Karl et al., 1993; Xie and Cao, 1996; Wilson and Luckman, 2002, 2003; Gou et al., 2008). The global warming over
349 the past few decades has been mainly caused by the rapid growth of night or minimum temperatures but not maximum
350 temperatures. Meanwhile, some differences between the reconstructed temperature values were well explained by a
351 comparison with similar areas.

352 We can conclude that the analysis shows that the reconstructed data is representative for large-scale regional
353 temperature variations (Fig. 7). At the same time, some cold and warm periods in our reconstruction and other
354 neighbored studies do not coincide (Fig. 8), which can be due to the reconstruction of other climatic parameters and
355 differing environmental conditions. So, we believe that these results can characterize regional climate variations and
356 provide reliable data for large-scale reconstructions for the northeastern portion of Eurasia, but their use for large-
357 scale regional reconstructions requires further research.

358 **4.3 Periodicity of climatic changes and their links to global climate processes**

359 Among the significant periodicities in the reconstructed temperature detected by the MTM analysis (Fig. 7), some
360 peaks were singled out: 2.3-year (95%), 2.5-year (99%), 2.9-year (99%), 3.0-year (99%), 3.3-year (95%), 3.7-year
361 (95%), 8.9-year (99%) short periods and 20.4-year (95%), 47.6-year (95%), and 188.7-year (99%) long periods. SSA
362 analysis shows significant near 3-year, 9-year, 20.4-year and 200-year periods.

363 The 3-year cycle may be linked with the El Niño-Southern Oscillation (ENSO). These high-frequency (2-7-year)
364 cycles (Bradley *et al.*, 1987) have also been found in other tree-ring-based temperature reconstructions in northeast
365 Asia (Zhu *et al.*, 2009; Li and Wang, 2013; Zhu *et al.*, 2016; Gao *et al.*, 2015). The 2–3-year quasi-cycles may also
366 correspond to the quasi-biennial oscillation (Labitzke and van Loon, 1999) and the tropospheric biennial oscillation
367 (Meehl, 1987). Despite the fact that many authors establish linkage between 2-7-year cycles and El Niño-Southern
368 Oscillation (ENSO) or quasi-biennial oscillation in northeastern Asia, we couldn't find significant correlation between
369 the August-December minimum temperature reconstruction and Nino3, but the analysis showed significant correlation
370 between the reconstruction and the temperature of Northern Hemisphere oceans. It probably mean that the temperature
371 variations are more associated with the influence of PDO than ENSO.

372 On the decadal timescale analysis showed 20-year cycles which may reflect processes influenced by Pacific Decadal
373 Oscillation (PDO, Mantua and Hare 2002) variability, which has been found at 15-25-yr and 50-70-yr cycles (Ma,
374 2007). Our analysis shows a significant correlation ($r=0.68$, $p<0.0001$) between reconstruction and the mean annual
375 PDO index of Mann *et al.* (2009) from 1900-2000. Taking into account that many researchers, who studied on the
376 territory of northeast Asia have also revealed these cycles in relation to the Korean pine, we hypothesize that the
377 Korean pine tree-ring series support the concept of long-term, multidecadal variations in the Pacific (e.g., D'Arrigo
378 *et al.*, 2001; Cook, 2002; Jacoby *et al.*, 2004; Liu *et al.*, 2009; Li, Wang, 2013; Willes *et al.*, 2014; Lu, 2016) and that
379 such variation or shifts have been present in the Pacific for several centuries. The PDO is a main index of major
380 variations in the North Pacific climate and ocean productivity (Mantua *et al.*, 1997; Jacoby *et al.*, 2004). In particular,
381 according to instrumental data analysis (Shatilina, Anzhina, 2008), the last warming of the northern part of the Pacific
382 Ocean (since 1970s) resulted in the intensive temperature increase and precipitation decrease in the southern part of
383 the Russian Far East.

384 We suppose that 9-year cycle may be related to solar activity, as, first of all, many authors showed influence of solar
385 activity on the climate variability (Bond *et al.*, 2001; Lean *et al.*, 1999; Lean, 2000; Mann *et al.*, 2009; Zhu *et al.*,
386 2016). Secondly, the significant correlation between of the August-December minimum temperature reconstruction
387 and TSI can be regarded as an additional evidence of this assumption. And, finally, there is a coincidence of the
388 reconstructed cold periods with the Maunder Minimum (1645–1715) and the Dalton minimum period centered in
389 1810. The solar activity influence in the region is traditionally associated with an indirect effect on the circulation of
390 the atmosphere (Erlykin *et al.*, 2009; Fedorov *et al.*, 2015). In the second half of the 20th century the solar radiation
391 intensity changes contributed to more intensive warming of the equatorial part of the Pacific Ocean and more active
392 inflow of warm air masses to the north (Fedorov *et al.*, 2015).

393 In spite, the fact that it is quite difficult to reveal for certain long-period cycles in a 486-year chronology, we
394 nonetheless revealed the 189-year cycle (MTM) or 200-year cycle (SSA analysis), which probably may possibly be
395 linked to the solar activity. Close periodicity is revealed in long-term climate reconstructions and is linked to the
396 quasi-200-year solar activity cycle in other study (Raspopov *et al.*, 2008; Raspopov *et al.*, 2009). Raspopov *et al.*
397 (2008) showed that in tree-ring based reconstructions the cycle varies from 180 to 230 years. Moreover, the high
398 correlation between the minimum temperatures reconstruction and TSI and also the revealed link between the
399 reconstructed temperatures and solar activity minima lead to suppose that the solar activity may be the driver of the
400 200-year cycle. Such climate cycling, linked not only to temperature but also to precipitation, is revealed for the
401 territories of Asia, North America, Australia, Arctic and Antarctic (Raspopov *et al.*, 2008). At the same time, the 200-
402 year cycle (*de-Vries* cycle) may often have a phase shift from some years to decades and correlates not only positively
403 but also negatively with climatic fluctuations depending on the character of the nonlinear response of the atmosphere-
404 ocean system within the scope of the region (Raspopov *et al.*, 2009). According to Raspopov *et al.* (2009), the study

405 area is in the zone that reacts with a positive correlation to solar activity, though the authors note that we should not
406 expect a direct response because of the nonlinear character of the atmosphere-ocean system reaction to variability in
407 solar activity (Raspopov et al., 2009). Taking into consideration this fact and that the cold and warm periods shown
408 in our reconstruction are slightly shifted compared with more continental areas and the whole Northern Hemisphere,
409 we can say that the reconstruction of minimum August-December temperatures reflects the global climate change
410 process in aggregate with the regional characteristics of the study area.

411 **Conclusions**

412 Using the tree-ring width of *Pinus koraiensis*, the mean minimum temperature of the previous August-December has
413 been reconstructed for the southern part of Sikhote-Alin Mountain Range, northeastern Asia, Russia, for the past 486
414 years. This dataset is the first climate reconstruction for this region, and for the first time for northeast Asia, we present
415 a reconstruction with a length exceeding 486 years.

416 Because explained variance of our reconstruction is about 39%, we believe that the result is noteworthy as it displays
417 the respective temperature fluctuations for the whole region, including northeast China, the Korean peninsula and the
418 Japanese archipelago. Our reconstruction is also in good agreement with the climatic reconstruction for the whole
419 Northern Hemisphere. The reconstruction shows good agreement with the cold periods described by documentary
420 notes in eastern China and Japan. All these comparisons prove that for this region, the climatic reconstruction based
421 on tree-ring chronology has a good potential to provide a proxy record for long-term, large-scale past temperature
422 patterns for northeast Asia. The results show the cold and warm periods in the region, which are conditional on global
423 climatic processes (PDO), and may reflect the influence of solar activity (the 9-11-year and 200-year solar activity
424 cycles). At the same time, the reconstruction highlights the peculiarities of the flows of global process in the study
425 area and helps in understanding the processes in the southern territory of the Russian Far East for more than the past
426 450 years. Undoubtedly, the results of our research are important for studying the climatic processes that have occurred
427 in the study region and in all of northeastern Asia and for situating them within the scope of global climatic change.

428

429 **Acknowledgements** This work was funded by Russian Foundation for Basic Research, Project 15-04-02185.

430 **References**

- 431 Anchukaitis K.J., D'Arrigo R.D., Andreu-Hayles L., Frank D., Verstege A., Curtis A., Buckley B.M., Jacoby G.C.,
432 and Cook E.R.: Tree-ring-reconstructed summer temperatures from Northwestern North America during the last
433 nine centuries. *J Clim.* 26, 3001-3012, doi: 10.1175/JCLI-D-11-00139.1, 2013.
- 434 Bard E., Raisbeck G., Yiou F. and Jouzel J.: Solar irradiance during the last 1200 years based on cosmogenic
435 nuclides. *Tellus B.*, 52, 985-992, 2000.
- 436 Bazarova V.B., Grebennikova T.A., and Orlova L.A.: Natural-environment dynamic within the Amur basin during
437 the neoglacial. *Geogr. Nat. Resour.*, 35(3), 275-283, doi: 10.1134/S1875372814030111, 2014.
- 438 Bond G., Kromer B., Beer J., Muscheler R., Evans M.N., Showers W., Hoffmann S., Lotti-Bond R., Hajdas I.,
439 Bonani G.: Persistent solar influence on north Atlantic climate during the Holocene. *Sci.*, 294, 2130-2136, 2001.
- 440 Borisova O.K.: Landscape-climatic changes in Holocene. *Reg. Res. Rus.*, 2, 5-20, 2014.
- 441 Bradley R.S., Diaz H.F., Kiladis G.N., Eischeid J.K.: ENSO signal in continental temperature and precipitation
442 records. *Nat.* 327, 497-501, 1987.

443 Dettinger M.D., Ghil M., Strong C.M., Weibel W., and Yiou, P.: Software expedites singular-spectrum analysis of
444 noisy time series, *Eos, Trans. American Geophysical Union* 76(2), 12, 14, 21, 1995.

445 Cook E.R., Kairiukstis L.A.: *Methods of dendrochronology: applications in the environmental sciences*. Kluwer
446 Academic Publishers, Dordrecht, 1990.

447 Cook E.R.: Reconstructions of Pacific decadal variability from long tree-ring records. *Eos Trans.* 83 (19) Spring
448 Meet. Suppl., Abstract GC42A-04, 2002.

449 Corona C., Guiot J., Edouard J.L., Chalié F., Büntgen U., Nola P. and Urbinati C.: Millennium-long summer
450 temperature variations in the European Alps as reconstructed from tree rings. *Clim. Past.*, 6, 379-400,
451 doi:10.5194/cp-6-379-2010, 2012.

452 Dai L.M., Qi L., Su D.K., Wang Q.W., Ye Y.J. and Wang Y.: Changes in forest structure and composition on
453 Changbai Mountain in Northeast China. *Ann. For. Sci.*, 68, 889-897, 2011.

454 Ding Y., Dai X.: Temperature Variation in China during the Last 100 years. *Meteorology*, 20, 19-26, 1994.

455 Durbin J. and Watson G.S.: Testing for serial correlation in least squares regression. *Biometrika*, 38, 159-178, 1951.

456 Efron B.: The jackknife, the bootstrap, and other resampling plans. *Pa. Soc. for Industrial and Appl. Mathem.*,
457 Philadelphia, 1982.

458 Efron B.: Bootstrap methods: another look at the jackknife. *Annals Statistics*, 7, 1-26, 1979.

459 Erlykin A.D., Sloan T. and Wolfendale W.: Solar activity and the mean global temperature. *Environ. Res. Lett.*, 4,
460 014006 (5pp), doi:10.1088/1748-9326/4/1/014006, 2009.

461 Fedorov V.M., Kononova N.K., Gorbunov R.V. and Gorbunova T.Yu.: Solar radiation and circulation processes in
462 the atmosphere of the Northern Hemisphere. *The complex systems*, 1(2), 58-71, 2015.

463 Fritts H.C.: *Tree rings and climate*. Academic Press Inc., London, 1976.

464 Fukaishi K. and Tagami Y.: An attempt of reconstructing the winter weather situations from 1720–1869 by the use
465 of historical documents. In: *Proceedings of the International Symposium on the Little Ice Age Climate*, Department
466 of Geography, Tokyo Metropolitan University, Tokyo, 194-201, 1992.

467 Ge Q., Zheng J., Hao Z., Liu Y. and Li M.: Recent advances on reconstruction of climate and extreme events in
468 China for the past 2000 years. *J Geogr Sci* 26(7), 827-854, doi: 10.1007/s11442-016-1301-4, 2016.

469 Ghil M., Allen R.M., Dettinger M.D., Ide K., Kondrashov D., Mann M.E., Robertson A., Saunders A., Tian Y.,
470 Varadi F. and Yiou P.: Advanced spectral methods for climatic time series. *Rev Geophys* 40(1), 3.1-3.41,
471 10.1029/2000RG000092, 2002.

472 Gou X., Chen F., Yang M., Gordon J., Fang K., Tian Q. and Zhang Y.: Asymmetric variability between maximum
473 and minimum temperatures in Northeastern Tibetan Plateau: evidence from tree rings. *Sci. China. Ser. D.* 51, 41-55,
474 2008.

475 Hirano J. and Mikami T.: Reconstruction of winter climate variations during the 19th century in Japan. *Int J*
476 *Climatol* 28, 1423-1434, doi:10.1002/joc.1632, 2007.

477 Holmes R.L.: Computer-assisted quality control in tree-ring dating and measurement. *Tree-ring Bull.* 43, 69-78,
478 1983.

479 Ishikawa Y., Krestov P.V. and Namikawa K.: Disturbance history and tree establishment in old-growth *Pinus*
480 *koraensis*-hardwood forests in the Russian Far East. *J. Veg. Sci.* 10, 439-448, 1999.

481 Jacoby G., Solomina O., Frank D., Eremenko N. and D'Arrigo R.D.: Kunashir (Kuriles) Oak 400-year
482 reconstruction of the temperature and relation to the Pacific Decadal Oscillation. *Palaeogeogr Palaeoclimatol*
483 *Palaeoecol*, 2009, 303-311, doi: 10.1016/j.paleo.2004.02.015, 2004.

484 Karl T.R., Jones P.D., Knight R.W., Kulas G., Plummer N., Razuvayev V., Gallo K.P., Lindsey J., Charlson R.J.,
485 and Peterson T.C.: A new perspective on recent global warming: asymmetric trends of daily maximum and
486 minimum temperature. *B. Am. Meteorol. Soc.*, 74, 1007-1023, 1993.

487 Kolesnikov B.P.: Korean pine forests of the [Russian] Far East. *Trudy DVF AN SSSR*. 2, 1-264, 1956 (In Russian).

488 Körner C. and Paulsen J.: A world-wide study of high altitude treeline temperatures. *J. Biogeogr.*, 31, 713-732,
489 doi:10.1111/j.1365-2699.2003.01043.x, 2004.

490 Kozhevnikova N.K.: Dynamics of weather-climatic characteristics and ecological function of small river basin. *Sib.*
491 *Ecol. J.*, 5, 93-703, 2009 (In Russian).

492 Kress A., Hangartner S., Bugmann H., Büntgen U., Frank D.C., Leuenberger M., Siegwolf R.T.W. and Saurer M.:
493 Swiss tree rings reveal warm and wet summers during medieval times. *Geophys. Res. Lett.*, 41, 1732-1737, doi:
494 10.1002/2013GL059081, 2014.

495 Labitzke K.G. and van Loon H.: *The Stratosphere: Phenomena, History and Relevance*. Springer, Berlin, 1999.

496 Lean J.: Evolution of the Sun's spectral irradiance since the Maunder Minimum. *Geophys. Res. L.*, 27(16), 2425-
497 2428, doi: 10.1029/2000GL000043, 2000.

498 Lean J. and Rind D.: Evaluating sun-climate relationships since the Little Ice Age. *J. Atmos. Sol. Terr. Phys.*, 61,
499 25-36, 1999.

500 Li M. and Wang X.: Climate-growth relationships of three hard- wood species and Korean pine and minimum
501 temperature reconstruction in growing season in Dunhua, China. *J. Nanjing. For. Univ.*, 37, 29-34, 2013.

502 Liu Y., Bao G., Song H., Cai Q. and Sun J.: Precipitation reconstruction from Hailar pine (*Pinus koraiensis* var.
503 *mongolica*) tree rings in the Hailar region, Inner Mongolia, China back to 1865 AD. *Paleogeogr Paleoclimatol*
504 *Paleoecol*, 282, 81-87, doi:10.1016/j.palaeo.2009.08.012, 2009.

505 Liu Q.J.: Structure and dynamics of the subalpine coniferous forest on Changbai mountain, China. *Plant. Ecol.* 132,
506 97-105, 1997.

507 Lu R., Jia F., Gao S., Shang Y. and Chen Y.: Tree-ring reconstruction of January-March minimum temperatures
508 since 1804 on Hasi Mountain, northwestern China. *J. Arid. Environ.*, 127, 66-73,
509 doi:10.1016/j.jaridenv.2015.10.020, 2016.

510 Lyu S., Li Z., Zhang Y. and Wang X.: A 414-year tree-ring-based April–July minimum temperature reconstruction
511 and its implications for the extreme climate events, northeast China. *Clim. Past.* 12, 1879-1888, doi:10.5194/cp-12-
512 1879-2016, 2016.

513 Ma Z.G.: The interdecadal trend and shift of dry/wet over the central part of north China and their relationship to the
514 Pacific Decadal Oscillation (PDO). *Chin. Sci. Bull.*, 52(12), 2130-2139, 2007.

515 Mann M.E. and Lees J.M.: Robust estimation of background noise and signal detection in climatic time series. *Clim.*
516 *Change*, 33, 409-445, 1996.

517 Mann M.E., Zhang Z., Rutherford S., Bradley R.S., Hughes M., Shindell D., Amman C., Faluvegi G. and Ni F.:
518 Global Signatures and Dynamical Origins of the Little Ice Age and Medieval Climate Anomaly. *Science*, 326, 1256-
519 1260, doi:10.1126/science.1177303, 2009.

520 Mantua N., Hare S.: The Pacific decadal oscillation. *J. Oceanogr.* 58(1), 35-44, 2002.

521 Meehl G.A.: The annual cycle and interannual variability in the tropical Pacific and Indian Ocean regions. *Mon.*
522 *Weather. Rev.*, 115, 27-50, 1987.

523 Melvin T.M. and Briffa K.R.: A 'signal-free' approach to dendroclimatic standardisation. *Dendrochronologia*, 26,
524 71-86, doi: 10.1016/j.dendro.2007.12.001, 2008.

525 Nishimura M. and Yoshikawa I.: Nippon Kyokoshi Ko, Maruzen, Tokyo, an archival collection of disasters in
526 Japan, 1936 (in Japanese)

527 Ohayama M., Yonenobu H., Choi J.N., Park W.K., Hanzawa M. and Suzuki M.: Reconstruction of northeast Asia
528 spring temperature 1784-1990. *Clim. Past.*, 9, 261-266, doi:10.5194/cp-9-261-2013, 2013.

529 Omelko A., Ukhvatkina O. and Zmerenetsky A.: Disturbance history and natural regeneration of an old-growth
530 Korean pine-broadleaved forest in the Sikhote-Alin mountain range, Southeastern Russia. *For. Ecol. Manag.* 360,
531 221-234, doi: 10.1016/j.foreco.2015.10.036, 2016.

532 Omelko A.M. and Ukhvatkina, O.N.: Characteristics of gap-dynamics of conifer-broadleaved forest of Southen
533 Sikhote-Alin (Russia). *Plant World Asian Russ.*, 1, 106-113, 2012.

534 Popa I. and Bouriaud O.: Reconstruction of summer temperatures in Eastern Carpathian Mountain (Rodna Mts,
535 Romania) back to AD 1460 from tree-rings. *Int. J. Climatol.*, 34, 871-880, doi: 10.1002/joc.3730, 2014.

536 Porter T.J., Pisaric M.F., Kokelj S.V. and DeMontigny P.: A ring-width-based reconstruction of June-July minimum
537 temperatures since AD 1245 from white spruce stands in the Mackenzie Delta region, northwestern Canada.
538 *Quaternary. Res.*, 80, 167-179, doi: 10.1016/j.yqres.2013.05.004, 2013.

539 Raspopov OM, Dergachev VA, Esper J, Kozyreva OV, Frank D, Ogurtsov M, Kolström T, Shao X (2008) The
540 influence of the de Vries (~200-year) solar cycle on climate variations: Results from the Central Asian
541 Mountains and their global link. *Palaeogeogr Palaeoclimatol Palaeoecol*, 259, 6-16. doi:
542 10.1016/j.palaeo.2006.12.017

543 Raspopov O.M., Dergachev V.A., Kozyreva O.V., Kolström T., Lopatin E.V. and Luckman B.: Geography of 200-
544 year climate periodicity and Long-Term Variations of Solar activity. *Reg. Res. Russ.*, 2, 17-27, 2009.

545 Razzhigaeva N.G., Ganzei L.A., Mokhova L.M., Makarova T.R., Panichev A.M., Kudryavtseva E.P., Arslanov
546 Kh.A., Maksimov F.E. and Starikova A.A.: The Development of Landscapes of the Shkotovo Plateau of Sikhote-
547 Alin in the Late Holocene. *Reg. Res. Russ.*, 3, 65-80, doi:10.15356/0373-2444-2016-3-65-80, 2016.

548 Ren F. and Zhai P.: Study on Changes of China's Extreme Temperatures During 1951-1990. *Sci. Atmos. Sin.*, 22,
549 217-227, 1998.

550 Sakaguchi Y.: Warm and cold stages in the past 7600 years in Japan and their global correlation. *Bull. Dep. Geogr.*
551 15, 1-31, 1983.

552 Shao X. and Wu X.: Reconstruction of climate change on Changbai Mountain, Northeast China using tree-ring data.
553 *Quaternary. Sci.*, 1, 76-83, 1997.

554 Shatilina T.A. and Anzhina G.I.: Features of atmospheric circulation and climate in the Far East (Russia) in the
555 beginning of 21 Century. *Izv. TINRO*, 152, 225-239, 2008 (In Russian).

556 Stokes M.A. and Smiley T.L.: Tree-ring dating. The University of Chicago Press, Chicago, London, 1968.

557 Tang H., Zhai P. and Wang Z.: On Change in Mean Maximum Temperature, Minimum Temperature and Diurnal
558 Range in China During 1951-2002. *Climatic Environ Res.*, 10, 728-735, 2005.

559 Thapa U.K., Shan S.K., Gaire N.P. and Bhujju D.R.: Spring temperatures in the far-western Nepal Himalaya since
560 1640 reconstructed from *Picea smithiana* tree-ring widths. *Clim dyn*, 45(7), 2069-2081, doi: 10.1007/s00382-014-
561 2457-1, 2015.

562 Wang H., Shao X.M., Jiang Y., Fang X.Q. and Wu S.W.: The impacts of climate change on the radial growth of
563 *Pinus koraiensis* along elevations of Changbai Mountain in northeastern China. *For. Ecol. Manag.*, 289, 333-340,
564 doi:10.1016/j.foreco.2012.10.023, 2013.

565 Wang X., Zhang M., Ji Y., Li Z., Li M. and Zhang Y.: Temperature signals in tree-ring width and divergent
566 growth of Korean pine response to recent climate warming in northeast Asia. *Trees* 31(2), 415-427, doi:
567 10.1007/s00468-015-1341-x, 2016.

568 Wang S., Liu J. and Zhou J.: The Climate of Little Ice Age Maximum in China. *J. Lake. Sci.*, 15, 369-379, 2003.

569 Wang W., Zhang J., Dai G., Wang X., Han S., Zhang H. and Wang Y.: Variation of autumn temperature over the
570 past 240 years in Changbai Mountain of Northeast China: A reconstruction with tree-ring records. *China. J. Ecol.*,
571 31, 787-793, 2012.

572 Wang Z., Ding Y., He J. and Yu J.: An updating analysis of the climate change in China in recent 50 years. *Ac*
573 *Meteorol Sin*, 62, 228-236, 2004.

574 Wigley T.M.L., Briffa K.R. and Jones P.D.: On the average value of correlated time series, with applications in
575 dendroclimatology and hydrometeorology. *J. Clim. Appl. Meteorol.*, 23, 201-213, 1984.

576 Wiles G.C., Solomina O., D'Arrigo R., Anchukaitis K.J., Gensiarovsky Y.V. and Wiesenberg N.: Reconstructed
577 summer temperatures over the last 400 year a based on larch ring widths: Sakhalin Island, Russian Far East. *Clim.*
578 *Dyn.*, 45, 397-405, doi: 10.1007/s00382-014-2209-2, 2014.

579 Wilson R.J.S. and Luckman B.H.: Tree-ring reconstruction of maximum and minimum temperatures and the diurnal
580 temperature range in British Columbia, Canada. *Dendrochronologia*, 20, 1-12, 2002.

581 Wilson R.J.S., Luckman B.H.: Dendroclimatic reconstruction of maximum summer temperatures from upper
582 treeline sites in Interior British Columbia, Canada. *Holocene*, 13, 851-861, doi:10.1191/0959683603hl663rp, 2003.

583 Xie Z. and Cao H.: Asymmetric changes in maximum and mini- mum temperature in Beijing. *Theor Appl Climatol*,
584 55, 151-56, 1996.

585 Yin H., Guo P., Liu H., Huang L., Yu H., Guo S. and Wang F.: Reconstruction of the October mean temperature
586 since 1796 at Wuying from tree ring data. *Adv. Clim. Change. Res.*, 5, 18-23, 2009.

587 Yin H., Liu H., Linderholm H.W. and Sun Y.: Tree ring density-based warm-season temperature reconstruction
588 since AD 1610 in the eastern Tibetan Plateau. *Palaeogeogr, Palaeoclimatol, Palaeoecol*, 426, 112-120, doi:
589 10.1016/j.palaeo.2015.03.003, 2015.

590 Young G.A.: Bootstrap: more than a stab in the dark. *Statistical. Sci.* 9, 382-415, 1994.

591 Zaiki M., Können G., Tsukahara T., Jones P., Mikami T. and Matsumoto K.: Recovery of nineteenth-century
592 Tokyo/Osaka meteorological data in Japan. *Int J Climatol*, 26, 399-423, doi:10.1002/joc.1253, 2006.

593 Zang C. and Biondi F.: Treeclim: an R package for the numerical calibration of proxy-climate relationships. *Ecogr.*
594 38, 001-006, doi: 10.1111/ecog.01335, 2015.

595 Zhang R.B., Yuan Y.J., Wei W.S., Gou X.H., Yu S.L., Shang H.M., Chen F., Zhang T.W. and Qin L.:
596 Dendroclimatic reconstruction of autumn-winter mean minimum temperature in the eastern Tibetan Plateau since
597 1600 AD. *Dendrochronologia*, 33, 1-7, doi: 10.1016/j.dendro.2014.09.001, 2015.

598 Zhao C., Ring G., Zhang Y., Wang Y.: Climate change of the Northeast China over the past 50 years. *J. Arid. Land.*
599 *Resour. Environ.*, 23, 25-30, 2009.

600 Zhu H.F., Fang X.Q., Shao X.M. and Yin Z.: Tree-ring-based February-April temperature reconstruction for
601 Changbai Mountain in Northeast China and its implication for East Asia winter monsoon. *Clim Past.*, 5, 661-666,
602 2009.

603 Zhu L., Li Z., Zhang Y. and Wang X.: A 211-year growing season temperature reconstruction using tree-ring width
604 in Zhanguangcai Mountains, Northeast China: linkages to the Pacific and Atlantic Oceans. *Int. J. Climatol.*, doi:
605 10.1002/joc.4906, 2016.

606 Zhu L., Li S., Wang X.: Tree-ring reconstruction of February-March mean minimum temperature back to 1790 AD
607 in Yichun, Northeast China. *Quaternary. Sci.*, 35, 1175-1184, doi: 10.11928/j.issn.1001-7410.2015.05.13, 2015.

608 **Tables**

609 **Table 1.** The sampling information and statistics of the signal-free chronology

	VUSr
Elevation (m a.s.l.)	700-900
Latitude (N), Longitude (E)	44°01'32'', E 134°13'15''
Core (live trees) / sample (dead trees)	25/20
Time period / length (year)	1451-2014 / 563
MS	0.253
SD	0.387
AC1	0.601
R	0.691
EPS	0.952
Period with EPS>0.85 / length (year)	1602-2014 / 412
Period with EPS>0.75 / length (year)	1529-2014 / 485
Skew/Kurtosis	0.982/5.204

610 MS – mean sensitivity, SD – standard deviation, AC1 – first-order autocorrelation, EPS – expressed population signal

611

612 **Table 2.** Calibration and verification statistics of the reconstruction equation for the common period 1971-2003 of

613 Bootstrap

Statistical item	Calibration	Verification (Bootstrap, 199 iterations)
r	0.62	0.62 (0.54-0.70)
R ²	0.39	0.39 (0.37-0.41)
R ² _{adj}	0.36	0.37 (0.37-0.40)
Standard error of estimate	1.20	1.11
F	18.76	18.54
P	0.0001	0.0001
Durbin-Watson	1.73	1.80

614

615 **Table 3.** Cold and warm periods based on the results of this study compared with other researches

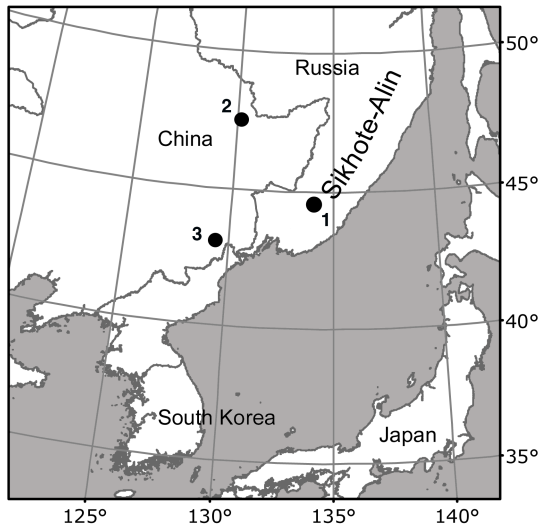
Period	Southern Sikhote-Alin (this study)	Laobai Mountain (Lyu et al., 2016)	Changbai Mountain (Zhu et al., 2009)
Cold	1535-1540 ¹ ; 1550-1555 ¹	*	*
	—	1605-1616	
	1643-1649; 1659-1667	1645-1677	*
	1675-1689	1684-1691	*
	1791-1801; 1807-1818	—	1784-1815
	1822-1827; 1836-1852		1827-1851
	1868-1887	—	1878-1889
	1911-1925	1911-1924; 1930-1942; 1951-1969	1911-1945
Warm	1560-1585 ¹	*	*

1600-1610 ¹ ; 1614-1618	—	*
1738-1743	—	—
1756-1759; 1776-1781	1767-1785	1750-1783
<i>1787-1793</i> **	1787-1793	—
<i>1795-1807</i> **	1795-1807	—
<i>1855-1865</i> **	—	1855-1877
1944-2014	1991-2008	1969-2009

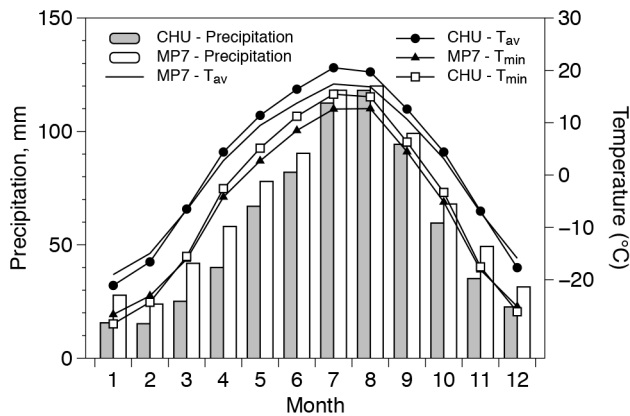
616 Note: *italic* ** – the periods which agreement with VUSr but not reliably for VUSr; * - the reconstruction not
617 covering this period; ¹ – uncertain periods, when chronology has EPS > 0.75 (AD 1529-1609).

618

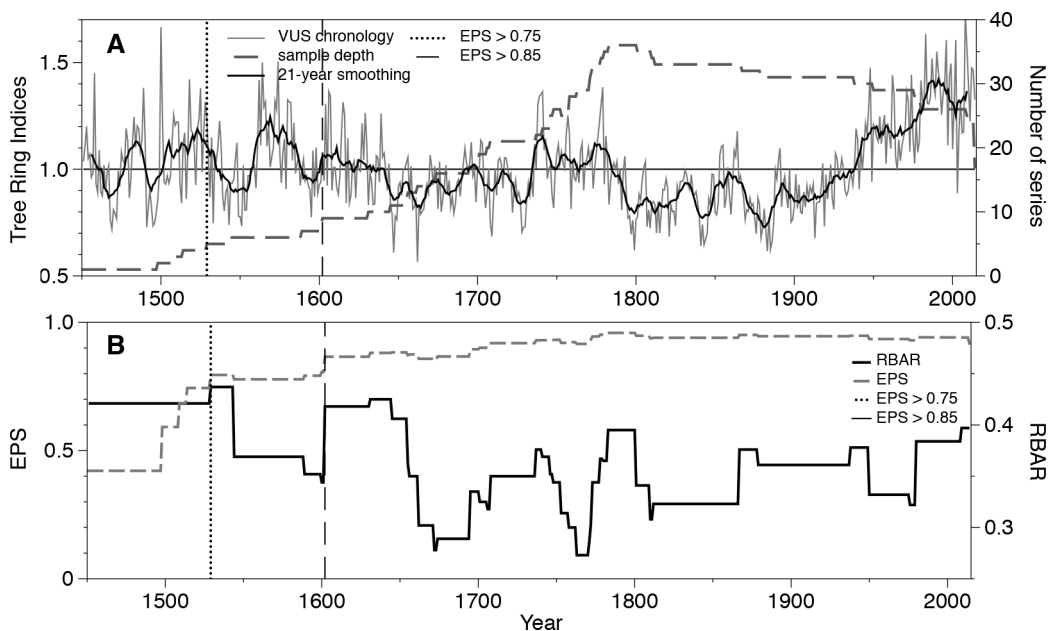
619 **Figure captions**



620
 621 **Figure 1:** Location of the study area on the Sikhote-Alin Mountains, Southeastern Russia (1) and sites of compared
 622 temperature reconstructions: April – July minimum temperature on Laobai Mountain by Lyu et al., 2016 (2), and
 623 February – April temperature established by Zhu et al. (2009) on Changbai Mountain (3).

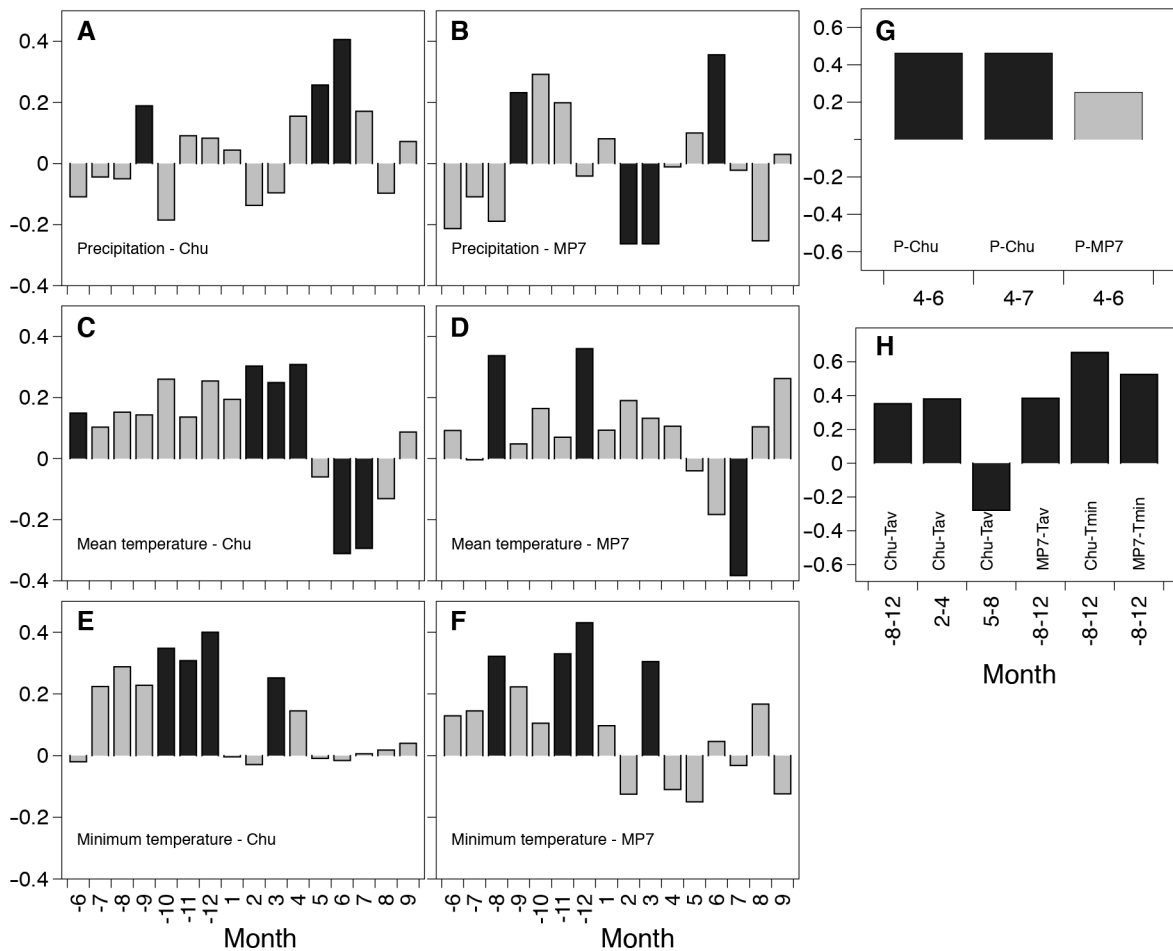


624
 625 **Figure 2:** Mean monthly (1936-2004), minimum temperature (1971-2003) and total precipitation (1936-2004) at
 626 Chuguevka and mean monthly, minimum temperature and total precipitation for VUS meteorological station (MP7)
 627 (1966-2000)

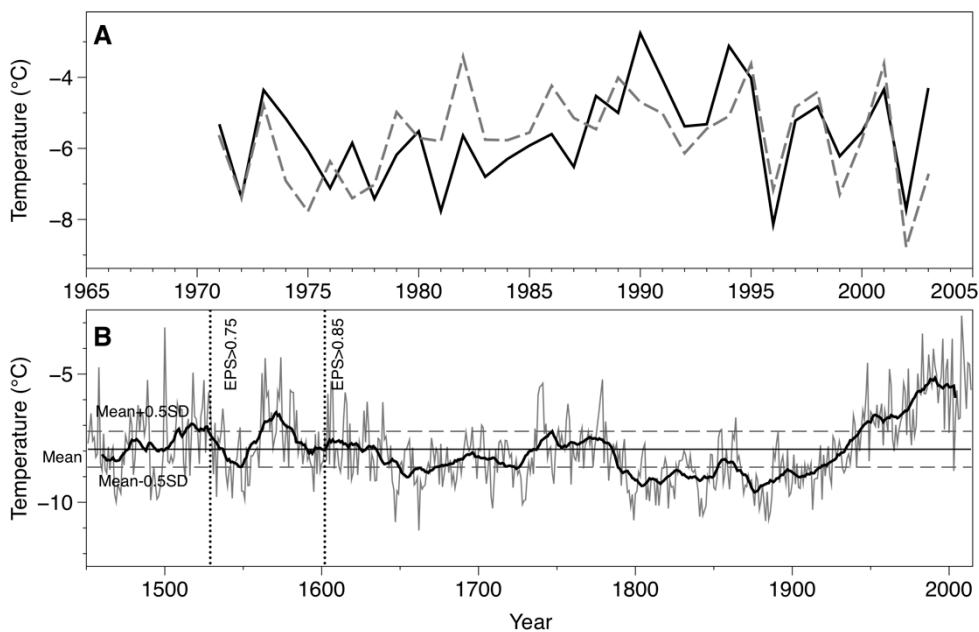


628

629 **Figure 3:** Variations of the VUS chronology and sample depth (a) and the expressed population signal (EPS) and
 630 average correlation between all series (R_{bar}) VUS chronology from AD 1451 to 2014 (b)

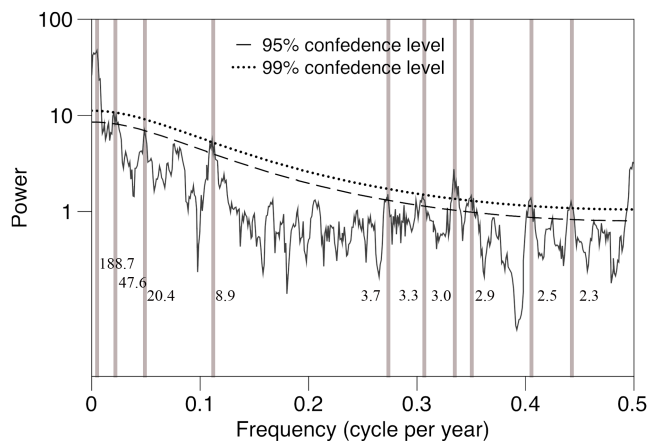


631
 632 **Figure 4:** Correlations between the monthly mean meteorological data and VUS chronology
 633 A, C, E – Chuguevka (Chu) and VUS chronology; B, D, F - VUS meteorological station (MP7) and VUS chronology;
 634 G – correlation coefficients between VUS chronology and the precipitation of different month combinations; H –
 635 correlation coefficients between VUS chronology and the temperature of different month combinations. The black
 636 bars are significant value.

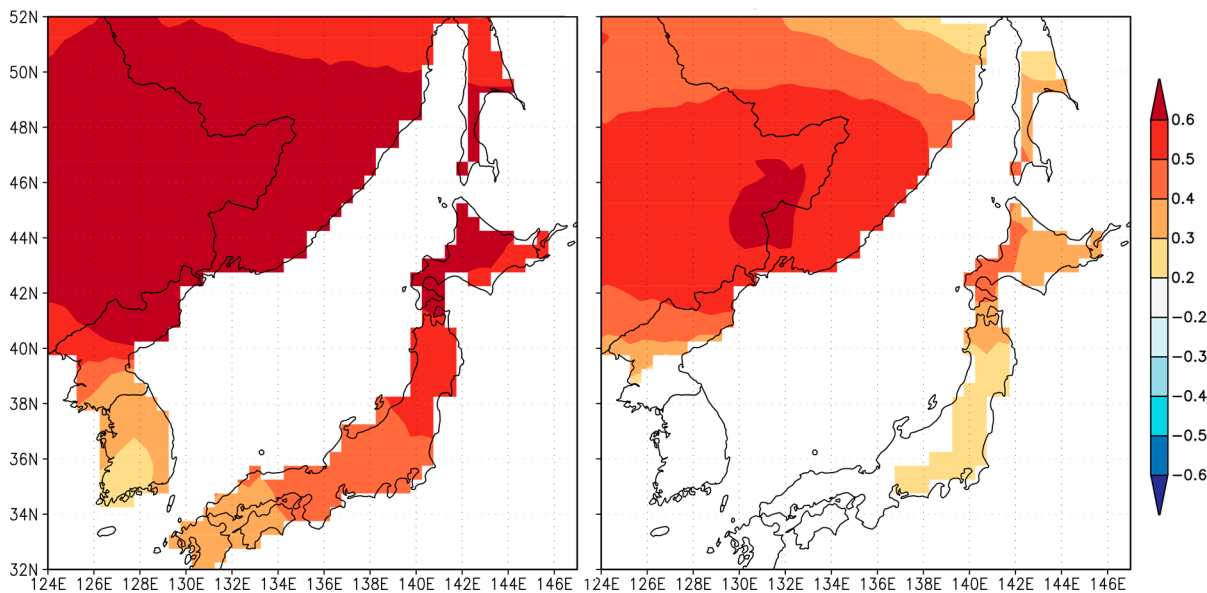


637

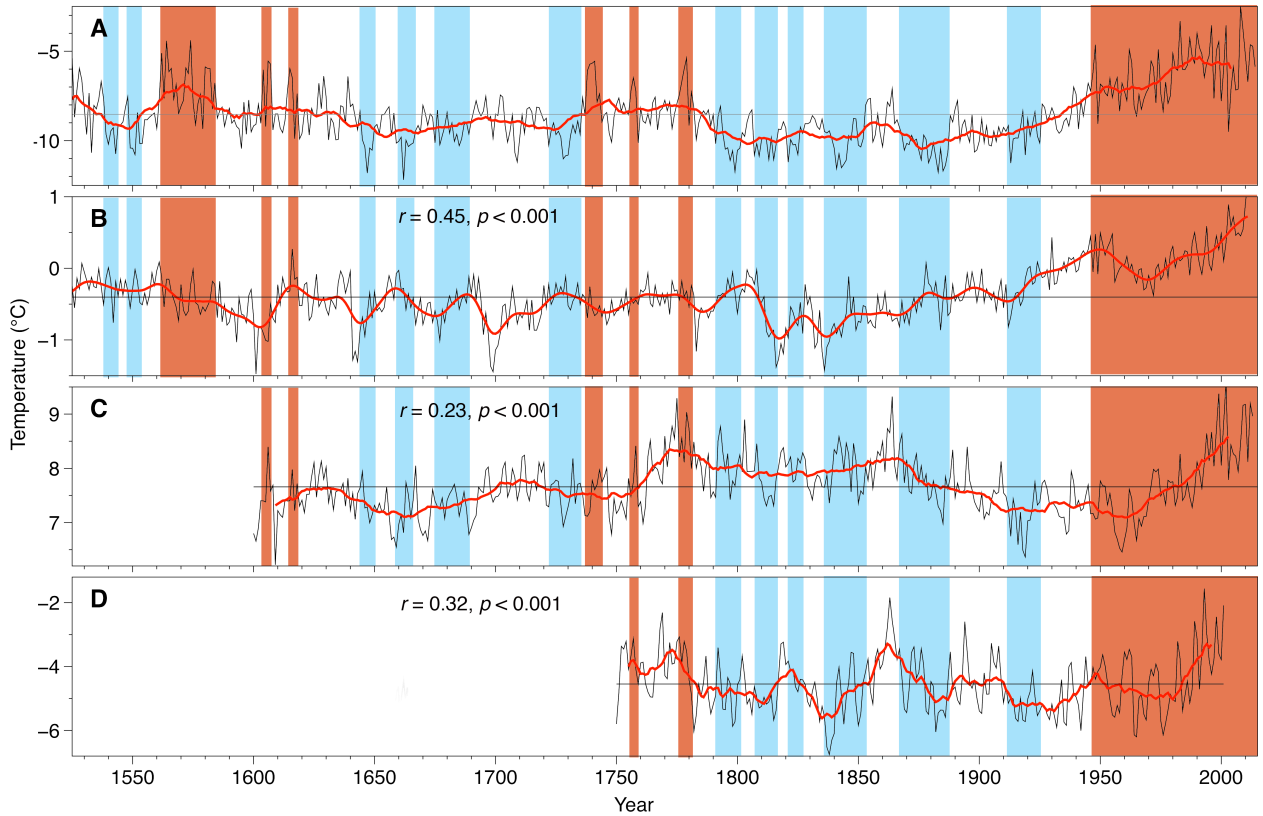
638 **Figure 5:** (a) Actual (black line) and reconstructed (dash line) August – December minimum temperature for the
 639 common period of 1971-2003; (b) reconstruction of August – December minimum temperature (VUSr) to Southern
 640 part of Sikhote-Alin for the last 563 years. The smoothed line indicates the 21-year moving average.



641
 642 **Figure 6:** The MTM power spectrum of the reconstructed August – December minimum temperature (VUSr) from
 643 1529 to 2014



644
 645 **Figure 7:** Spatial correlations between the observed (a) and reconstructed (b) August – December minimum
 646 temperature (VUS) in this study and regional gridded annual minimum temperature from CRU TS 4.00 over their
 647 common period 1960–2003 ($p < 10\%$).



649

650

651

652

653

654

Figure 8: (a) August-December mean minimum temperature reconstructed (VUSr) on southern part of Sikhote-Alin, (b) Northern Hemisphere extratropical temperature (Willes et al., 2016), (c) April – July minimum temperature on Laobai Mountain by Lyu et al., 2016, and (d) February – April temperature established by Zhu et al. (2009) on Changbai Mountain. Black lines denote temperature reconstruction values, and red color lines indicate the 21-year moving average; red and blue fields – warm and cold period consequently (in this study)